

The Galactic distribution of X-ray binaries and its implications for compact object formation and natal kicks

Serena Repetto^{1,2*}, Andrei P. Igoshev¹, Gijs Nelemans^{1,3}

¹Department of Astrophysics/IMAPP, Radboud University, P.O. Box 9010, 6500 GL Nijmegen, The Netherlands

²Physics Department, Technion - Israel Institute of Technology, Haifa, Israel 32000

³Institute for Astronomy, KU Leuven, Celestijnenlaan 200D, 3001 Leuven, Belgium

6 January 2017

ABSTRACT

The aim of this work is to study the imprints that different models for black hole (BH) and neutron star (NS) formation have on the Galactic distribution of X-ray binaries (XRBs) which contain these objects. We find that the root mean square of the height above the Galactic plane of BH- and NS-XRBs is a powerful proxy to discriminate among different formation scenarios, and that binary evolution following the BH/NS formation does not significantly affect the Galactic distributions of the binaries. We find that a population model in which at least some BHs receive a (relatively) high natal kick fits the observed BH-XRBs best. For the NS case, we find that a high NK distribution, consistent with the one derived from the measurement of pulsar proper motion, is the most preferable. We also analyse the simple method we previously used to estimate the minimal peculiar velocity of an individual BH-XRB at birth. We find that this method may be less reliable in the bulge of the Galaxy for certain models of the Galactic potential, but that our estimate is excellent for most of the BH-XRBs.

Key words: X-rays: binaries – supernovae: general – Galaxy: dynamics – binaries: general – black hole physics – stars: neutron

1 Introduction

The formation mechanism of compact objects, neutron stars (NSs) and black holes (BHs), is an unsolved problem in high-energy astrophysics. A model for the formation of such objects requires to perform physically-motivated simulations of the core-collapse supernova, which is computationally challenging (see e.g. Fryer & Warren 2002; Burrows et al. 2012; Janka 2012). Another possible way to investigate the formation of NSs and BHs is to study the birth and evolution of X-ray binaries (XRBs) hosting a BH or a NS accreting from a stellar companion. The orbital parameters, peculiar velocities and Galactic position of these binaries directly follow from their evolutionary history, and are affected in particular by the conditions at the moment of compact object formation (see e.g. Brandt & Podsiadlowski 1995; Kalogera et al. 1998; Nelemans et al. 1999; Nelemans 2007).

The measurement of pulsar proper motions (see e.g. Lyne & Lorimer 1994; Hansen & Phinney 1997; Hartman 1997; Hobbs et al. 2005), combined with the study of NS-XRBs (e.g. Johnston et al. 1992; Kaspi et al. 1994; Fryer & Kalogera 1997; Kolb et al. 2000; Pfahl et al. 2002), has exposed evidence that some NSs receive a low velocity, whereas others a high velocity at formation (so called *natal kicks*, NKs). The prevailing idea is that NSs are

formed either in a standard core-collapse supernova (SN), or in a less energetic type of SN expected for star with small cores. The latter can take place either as an electron-capture SN or as an iron core-collapse SN with a small iron-core mass (Podsiadlowski et al. 2004; Takahashi et al. 2013; Tauris et al. 2015; Janka 2016). For the case of BHs, observations are rather scarce and patchy, thus it is not yet possible to discriminate between different models of BH formation (Mirabel & Rodrigues 2003; Jonker & Nelemans 2004; Willems et al. 2005; Dhawan et al. 2007; Fragos et al. 2009; Miller-Jones et al. 2009; Wong et al. 2012; Wong et al. 2014; Repetto & Nelemans 2015; Mandel 2016). In this paper, one of our goals is to investigate whether the observed Galactic distribution of XRBs hosting a BH (BH-XRBs) can reveal something about how BHs are formed. The main underlying idea is that any offset of a BH-XRB from the Galactic plane (assumed as birth place) is a signature of some peculiar velocity of the system with respect to the circular Galactic motion. The magnitude of such velocity gives clues on the SN mechanism, in particular on the magnitude of the NK at birth (Jonker & Nelemans 2004; Repetto et al. 2012). The idea of using the Galactic position and/or line of sight velocities of a population of XRBs to investigate the formation of compact objects was employed previously for the NS case (see e.g. Brandt & Podsiadlowski 1995; Johnston 1996).

We covered the topic of BH formation in two previous works. In Repetto et al. (2012), we followed the Galactic trajectories of

* E-mail: repetto@physics.technion.ac.il

a simulated population of BH-XRBs, and investigated which NK distribution gives rise to the observed z -distribution of BH-XRBs (where z is the height above the Galactic plane). The aim was to discriminate between *high* and *reduced* NKs for BHs. High NKs are larger than the NK expected in a standard formation scenario for BHs, in which the BH forms via fallback of material on to the proto-NS and the NK is caused by asymmetries in the SN ejecta. In the standard scenario, the NK would conserve the linear-momentum and roughly scale as the NK received by the NS multiplied by the ratio between the mass of the BH and the mass of the NS. We call these kicks as *reduced* or *momentum-conserving* NKs. If the NS receives a NK of the order of 300 km/s, a $10 M_\odot$ BH would get a NK of ≈ 40 km/s. We define *high* NKs as $\gtrsim 100$ km/s. In Repetto et al. (2012), we found that high NKs, comparable to NS NKs, were required. In Repetto & Nelemans (2015), we combined the information from the kinematics and binary evolution of a subset of BH-XRBs to find evidence both for low and high NKs. In this Paper, we aim at complementing and extending those previous studies. Following up on the work by van Paradijs & White (1995) and White & van Paradijs (1996), Jonker & Nelemans (2004) found that the root-mean-square (rms) value of the height above the Galactic plane of BH-XRBs is similar to that of NS-XRBs, suggesting that BHs could also receive a *high* kick at formation, or even one as high as NSs. In this work, we develop this idea further. We build synthetic populations of BH- and NS-XRBs and we model their binary evolution and their kinematics in the Galaxy, to investigate whether different assumptions on compact object formation (such as a different distribution for the NK and/or a different amount of mass ejected in the SN) have an imprint on the observed Galactic distribution of BH- and NS-XRBs, and we quantify these effects.

Furthermore, we will dedicate part of this work to discuss a method we previously employed to calculate the minimum peculiar velocity at birth of individual BH-XRBs (Repetto et al. 2012; Repetto & Nelemans 2015). The difference of the Galactic potential value between the observed position (R, z) and its projection on to the Galactic plane was used to analytically derive a lower limit for the peculiar velocity at birth. This method has been recently challenged by Mandel (2016). We investigate how robust our estimate is, i.e. how close this estimate is to the true value of the minimal peculiar velocity at birth, how this estimate scales with the distance from the Galactic centre, and how it varies for different choices of the Galactic potential.

The paper is structured as follows. In Section 2 we study our estimate for the peculiar velocity at birth of individual BH-XRBs. In Section 3 we build synthetic populations of BH- and NS-XRBs for different assumptions on the compact object formation. In Section 4 we look at the Galactic distributions of these synthetic binaries while investigating how they differ, and inferring which NK distribution fits best the observed Galactic position of NS- and BH-XRBs. In Section 5 we discuss our findings and in Section 6 we draw our conclusions.

2 Intermezzo

2.1 On the estimate of the peculiar velocity at birth

XRBs are thought to originate from binary progenitors born in the Galactic plane, the birth-place of most massive stars (Brandt & Podsiadlowski 1995). When the compact object forms, the binary typically acquires a peculiar velocity. The mass ejection in the SN

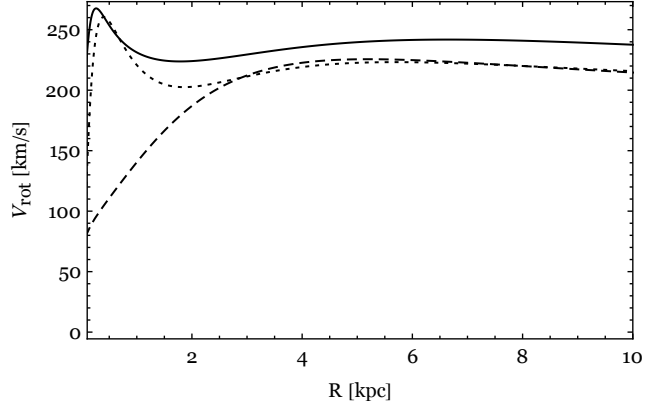


Figure 1. Rotation curve for the Galactic potentials used in this work: Bovy (2015) (dashed line), Paczynski (1990) (dotted line), Irrgang et al. (2013) (solid line).

imparts a recoil velocity to the binary; the NK adds up vectorially to this velocity, giving the total peculiar velocity of the binary, \vec{V}_{pec} . Such a systemic velocity adds up vectorially to the local Galactic rotation and probably has no preferential orientation. The full 3D velocity is measured only for a handful of BH-XRBs (see Miller-Jones 2014). For these, the integration of the orbit backwards in time can in principle provide an estimate for \vec{V}_{pec} at birth. However, uncertainty in the distance and differences in the Galactic potential can prevent a unique determination of the initial position (see e.g. Fragos et al. 2009; Miller-Jones et al. 2009). When the full 3D peculiar velocity is not known, one can estimate \vec{V}_{pec} at birth using a simple model. For an object located at Galactic height z^\dagger , we expect a trajectory purely perpendicular to the plane to be the one which minimises the initial \vec{V}_{pec} . In our previous works Repetto et al. (2012) and Repetto & Nelemans (2015), we estimated the minimum peculiar velocity at birth of a BH-XRB employing energy conservation along such trajectory, and assuming that the maximum height z from the plane is the observed one. We get:

$$V_{\text{pec},\text{min}} = \sqrt{2[\Phi(R_0, z) - \Phi(R_0, 0)]}, \quad (1)$$

where $\Phi(R, z)$ is a model for the Galactic potential, R_0 is the measured distance of the binary from the Galactic centre projected on to the Galactic plane, and z is the current height above the plane.

Recently Mandel (2016) argued that the difference in the gravitational potential between the observed location and its projection on to the Galactic plane is not an accurate estimate of the required minimum peculiar velocity at birth. He suggests that there are always possible trajectories different from a purely perpendicular one which require a lower V_{pec} at birth than the one estimated through equation 1 to reach the same offset from the Galactic plane.

We check the validity of our estimate for the peculiar velocity at birth, $V_{\text{pec},\text{min}}$, for high- z sources, performing a Monte Carlo simulation using the Python package for galactic dynamics `galpy`[†] (Bovy 2015). We simulate 1.1×10^7 points, whose initial conditions are set as follows: 1) the initial position is at $(R, z) = (R_i, 0)$, where R_i is uniformly distributed between 0 and 18 kpc; 2) the initial peculiar velocity V_{pec} is uniform between 0 and 500 km/s; 3) the orientation of this velocity is uniformly distributed over a

[†] Throughout this work, we use a reference frame centered at the Galactic centre and cylindrical coordinates with R : the distance from the Galactic centre, and z : the height above the Galactic plane.

[‡] Available at <https://github.com/jobovy/galpy>

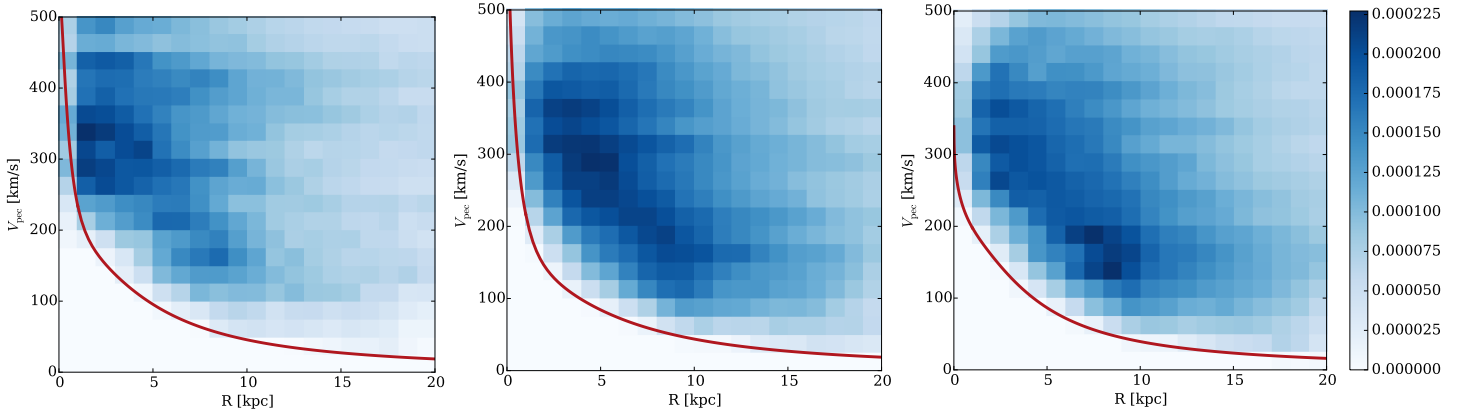


Figure 2. Density plots showing the fraction of systems in every bin of initial peculiar velocity V_{pec} and distance from the Galactic centre R (projected on to the Galactic plane) of points which reach a height above the Galactic plane greater than 1 kpc. The red line shows our analytical estimate $V_{\text{pec},\text{min}}$. We use three different potentials; from left to right: Paczynski (1990), Irrgang et al. (2013), Bovy (2015).

sphere. We note that since we are only interested in the minimum value of V_{pec} , the shape of the assumed velocity distribution is not important. We add the circular motion in the Galactic disc to the 3D peculiar velocity \vec{V}_{pec} . We integrate the orbits in the Galaxy for 5 Gyr, using a 4th-order Runge-Kutta integrator, and we check for conservation of energy over the trajectory making sure that the relative error on the energy is less than 10^{-5} at the final step. We record the positions (R, z) 500 times over the orbit sampling from constant time steps, along with the initial peculiar velocity V_{pec} . From the simulated points, we select only those ones located at $z^2 > 1$ at the sampled times, to represent high- z sources. We perform the simulation for three different choices of the Galactic potential: model 2 of Irrgang et al. (2013)[§], Paczynski (1990), and the MWPotential2014 potential from Bovy (2015), which are all multi-component potentials consisting of disc, bulge, and halo. The Paczynski (1990) potential is made up of two Miyamoto-Nagai potentials for disc and bulge, and one pseudo-isothermal potential for the halo. The Bovy (2015) potential is made up of a power-law density profile with an exponential cut-off for the bulge, a Miyamoto-Nagai Potential for the disc, and a Navarro-Frenk-White profile for the halo. The Irrgang et al. (2013) potential is composed of two Miyamoto-Nagai potentials and a Wilkinson-Evans potential for the halo. We show the rotation curve of each of the three potentials in Figure 1. Irrgang et al. (2013) is the potential used by Mandel (2016); Paczynski (1990) is the one we adopted in Repetto et al. (2012); the MWPotential2014 is a realistic model for the Milky Way potential favoured by Bovy (2015). We present the results of this simulation in Figure 2. The red line is our estimate for the peculiar velocity taking $z = 1$ kpc in equation 1 and it follows the lower edge of the simulated points.

Figure 2 shows that our analytical estimate (eq. 1) successfully describes the value and trend of the minimal peculiar velocity as a function of the Galactocentric distance.

In order to better quantify the goodness of our estimator $V_{\text{pec},\text{min}}$, we compute the ratio $\gamma = V_{\text{pec}}/V_{\text{pec},\text{min}}$ using 1 kpc-wide bins in R , for those points which reach a height above the Galactic plane along their orbit in the range $|z| = (1, 1.1)$ kpc. The velocity V_{pec} is the actual initial peculiar velocity which we showed in Figure 2. We plot γ in Figures 3, 4, 5, for the three different po-

tentials. $V_{\text{pec},\text{min}}$ is an excellent estimator for $R > 1$ kpc, since at these radii γ is equal or greater than 1. It is less robust in the inner part of the bulge for the Paczynski (1990) and Irrgang et al. (2013) potentials, but not in the MWPotential2014 potential, that is fit to the most recent dynamical constraints on the Milky Way and has a more realistic bulge model (Jo Bovy, private communication). In the bulge region, our estimate is steeper than the real minimal peculiar velocity for the first two potentials, i.e., it varies strongly for small variation in R . This can be seen in Figure 6, where for every position (R, z) we show as a density map the real minimal peculiar velocity at birth necessary to reach that position. We integrated 10^4 orbits for 5 Gyr and using as potential the one in Irrgang et al. (2013). The contour lines show our analytical estimate $V_{\text{pec},\text{min}}$; the discrepancy between the two velocities is evident in the inner region of the Galaxy.

Figures 3, 4, 5 also show an increase of the average value of γ with larger distances R . This is an artefact caused by our choice of the V_{pec} initial distribution (uniform between 0 – 500 km/s), as the numerator in the ratio γ can take all the values between $\approx V_{\text{pec},\text{min}}$ and 500 km/s.

From our extensive analysis, we find that the estimate $V_{\text{pec},\text{min}}$ accurately represents the real minimal value for the peculiar velocity at distances from the Galactic centre $\gtrsim 1$ kpc, and can be safely applied to estimate the peculiar velocity at birth of XRBs born in the Galactic plane.

2.2 Effect of a different choice of the Galactic potential with an application to the observed BH-XRBs

The estimate $V_{\text{pec},\text{min}}$ is a function of the potential used, in particular in the bulge, as can be seen in Figure 7, where we show $V_{\text{pec},\text{min}}$ for the Paczynski (1990), Irrgang et al. (2013) and Bovy (2015) potentials, and assuming $z = 1$ kpc in eq. 1. Additionally, from Figures 3, 4, 5, we note that the fraction of systems with $\gamma < 1$ in the region $R = [0, 1]$ kpc also strongly depends on the potential. The minimum values γ_{min} are: 1.01, 0.72, 0.61 for Bovy (2015), Irrgang et al. (2013), Paczynski (1990) potential respectively, where these lower limits are defined such that 95% of the points in the same bin have a value larger than the lower limit.

Figure 2 also shows that the Galactic bulge ($R \lesssim 1$ kpc) is much less populated (an order of magnitude fewer systems than in regions at larger distance from the Galactic center). There are two

[§] When referring to the Irrgang et al. (2013) Galactic potential, we will hereafter refer to their model 2.

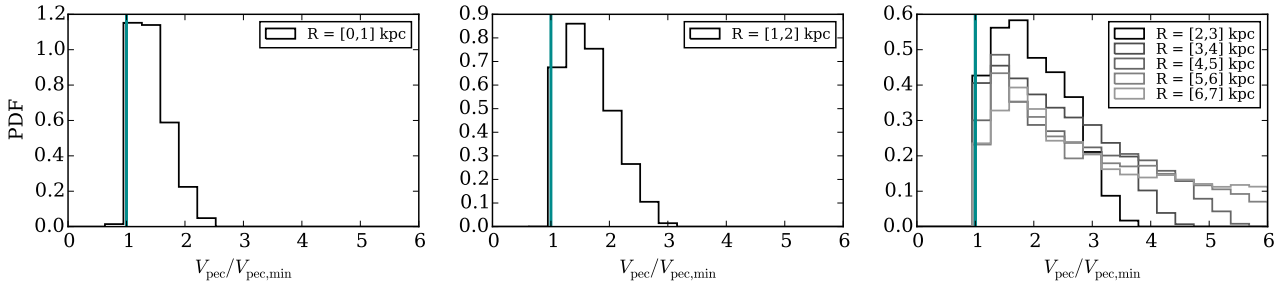


Figure 3. Ratio $V_{\text{pec}}/V_{\text{pec,min}}$ for points such that the observed position is at $1 < z < 1.1$ kpc. Each panel shows a different R-bin. The Galactic potential is from Bovy (2015).

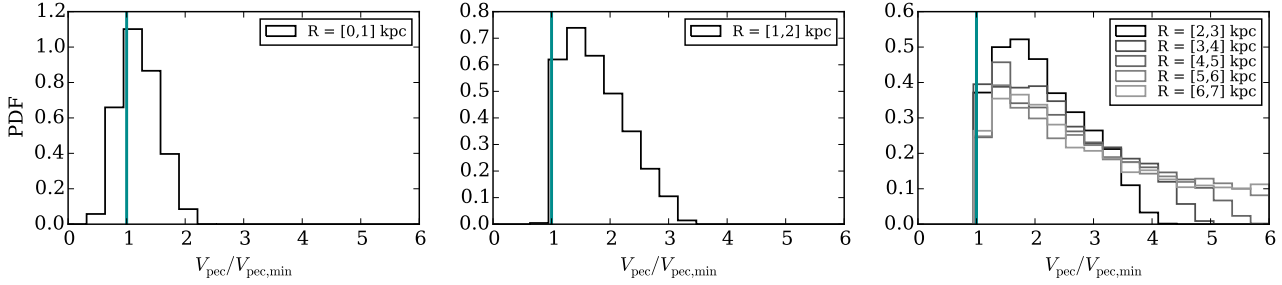


Figure 4. Ratio $V_{\text{pec}}/V_{\text{pec,min}}$ for points such that the observed position is at $1 < z < 1.1$ kpc. Each panel shows a different R-bin. The Galactic potential is from Irrgang et al. (2013).

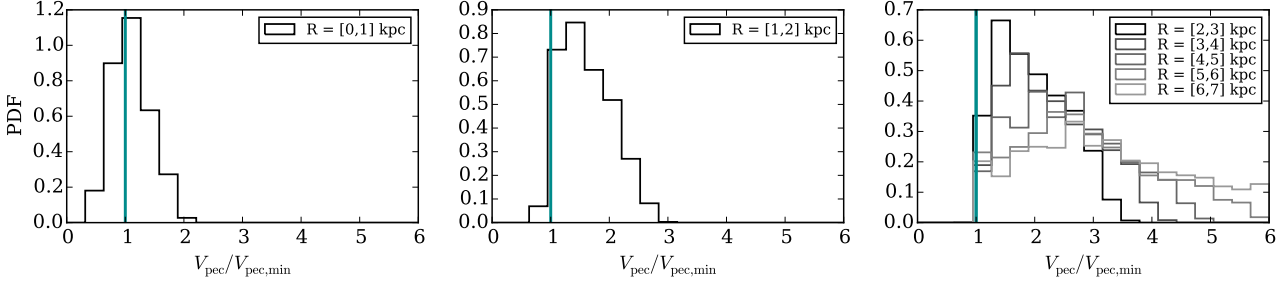


Figure 5. Ratio $V_{\text{pec}}/V_{\text{pec,min}}$ for points such that the observed position is at $1 < z < 1.1$ kpc. Each panel shows a different R-bin. The Galactic potential is from Paczynski (1990).

reasons for this: i) the bulge volume is small; ii) it is unlikely for a binary born in the Galactic disc to overcome the strong potential well in its motion towards the Galactic bulge. The inaccuracy of our analytical estimate in the bulge region affects only the source H1705-250, which is the only BH-XRB located close enough to the Galactic centre (see Table 2), at $(R, z) \approx (0.5, 1.3)$ kpc (Remillard et al. 1996). Without a measurement of its 3D peculiar velocity, it is impossible to discriminate between a birth in the disc or a birth in the bulge (hence close to its observed position). More in general, bulge sources are not suitable for estimating the peculiar velocities at birth, since the current view on bulge formation is that it was not formed in situ. The bulge population is thought to come from the disc through dynamical instabilities (Gerhard 2015), with most of its mass coming from major and minor merger events with satellite galaxies (De Lucia et al. 2011).

We compute the minimum peculiar velocity at birth for the seven short-period BH-XRBs studied by Repetto & Nelemans (2015), using the three Galactic potentials (see Table 1). We add to this sample two other short-period BH-XRBs which we did not consider in Repetto & Nelemans (2015) (XTE J1650-500 and XTE J1859+226), due to the lack of a strong constraint on the BH mass

Table 1. Minimum peculiar velocity at birth for short-period BH-XRBs. The velocities are estimated using three different Galactic potentials and are given in km/s. The numbers in parenthesis for H 1705-250 correspond to correcting the estimates for the inaccuracy of our analytical estimate in the bulge of the Galaxy (see Text).

Source	V _{pec,min} [km/s]			
	Bovy	Pac.	Irrgang	Repetto et al. 2015
XTE J1118+480	62	70	68	72
GRO J0422+32	20	25	22	25
GRS 1009-45	34	40	37	41
1A 0620-00	8	10	8	10
GS 2000+251	12	15	12	15
Nova Mus 91	44	51	46	52
H 1705-250	259 (262)	363 (158)	350 (186)	402
XTE J1650-500	17	21	16	-
XTE J1859+226	61	68	68	-

(Casares & Jonker 2014). For H 1705-250, we put in parenthesis the velocity $V_{\text{pec,min}}$ multiplied by the factor γ found above.

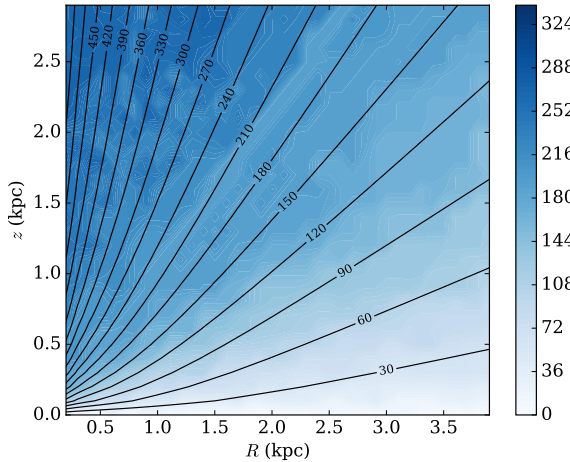


Figure 6. Density map showing with color coding the minimal value for the peculiar velocity at birth V_{pec} of simulated points which reach that position (R, z) . The contour lines show our analytical estimate $V_{\text{pec},\text{min}}$ at that position. The estimate differs strongly from the real value in the bulge region (each solid line differs by ± 30 km/s from the closest-neighbouring one). The potential used is from Irrgang et al. (2013).

We have found an error in the halo component of the Paczynski (1990) potential that we used for the computation of $V_{\text{pec},\text{min}}$ in Repetto & Nelemans (2015). This mostly affects the bulge source H 1705-250, whereas the other six sources are not greatly affected (compare third and last column in Table 1).

Accounting for the thickness of the Galactic disc instead of assuming a birth place at $z = 0$ does not significantly affect the minimal peculiar velocity (see Belczynski et al. 2016).

Mandel (2016) used the source H 1705-250 to conclude that the difference in the Galactic potential between the observed position and the projection of this position on to the Galactic plane is not a conservative estimate of the minimal initial velocity of the binary. They show an example of a trajectory for H 1705-250 which starts from the Galactic plane and ends at the observed position for an initial velocity of ≈ 230 km/s, lower than the value provided by eq. 1 (see Table 1). We agree with his conclusion, but only as far as sources close (or in) the bulge are concerned. On the contrary, for sources located at $R \gtrsim 1$ kpc, our analytical estimate perfectly matches the real minimal velocity. In Repetto & Nelemans (2015) we used the high minimal velocity at birth for XTE J1118+480 and H 1705-250 to claim that at least two out of the seven BH-XRBs we considered were consistent with a high (or relatively high) NK. This holds true with our current revision of the minimal velocities at birth, and we find another BH-XRB that is potentially consistent with a relatively high NK: XTE J1859+226.

The velocities we have been dealing so far with are *minimal* velocities, and do not necessarily correspond to *expected (realistic)* velocities. In what follows, we study the latter.

3 A Binary Population Synthesis of BH- and NS-XRBs

In this part of the work, instead of dealing with the minimal peculiar velocities, we deal with the expected peculiar velocities. We perform a binary population synthesis study of BH- and NS-XRBs, starting just before the BH/NS formation, varying the conditions at the formation of the compact object. The goal is to investigate the impact that different BH and NS formation assumptions have

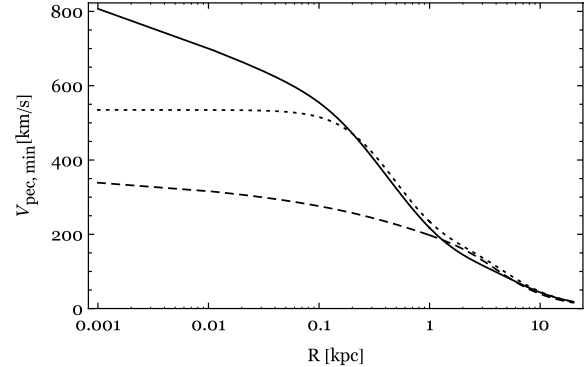


Figure 7. Analytical estimate $V_{\text{pec},\text{min}}$ for the peculiar velocity at birth as a function of the distance from the Galactic centre R (projected on to the Galactic plane) for the three different Galactic potentials used in this work: Bovy (2015) (dashed line), Paczynski (1990) (dotted line), Irrgang et al. (2013) (solid line). We assumed $z = 1$ kpc.

on the Galactic distribution of XRBs containing a NS or a BH. We assume that the binaries are formed in the Galactic thin disc, where most of the massive stars reside (Urquhart et al. 2014). In this study, we do not account for the possibility that a few systems could have been formed in the halo (i.e. in star clusters that have now been dissolved), and neither of the possibility that a few systems could have been ejected from globular clusters (GCs) via N-body interactions. GCs seem to be very efficient in producing NS low-mass X-ray binaries (NS-LMXBs), as 10% of all NS-LMXBs are found in globular clusters, which contain only $\sim 0.1\%$ of all the stars in the Galaxy (Irwin 2005). Such an investigation is, however, outside the scope of this paper.

We take different models for the formation of the compact object. The NK is drawn either from a Maxwellian distribution peaked at 40 km/s (with $\sigma \approx 28$ km/s) representing a low-NK, or from a Maxwellian distribution peaked at 100 km/s (with $\sigma \approx 71$ km/s) representing a high-NK. We assume a certain amount of mass ejection in the SN, M_{ej} . BHs are thought to form either via prompt collapse of the progenitor star or via partial fallback of the SN ejecta onto the proto-NS (see Fryer & Kalogera 2001). In our models, the progenitors of BHs either do not eject any mass at collapse, or they eject $4 M_{\odot}$. Stars with a ZAMS-mass larger than $\approx 25 M_{\odot}$ are thought to leave a BH behind (see e.g. Fryer & Kalogera 2001; Tauris & van den Heuvel 2006). For a progenitor of mass $25 - 60 M_{\odot}$, the helium core mass (which collapses into a BH) is between $\approx 8 - 11 M_{\odot}$ (Belczynski et al. 2008), which motivates our (conservative) choice for M_{ej} . For the previous models, we assume a BH mass of $8 M_{\odot}$ (which is the typical mass for BHs in our Galaxy; Özel et al. 2010). We also picture a higher-mass helium star ($M_{\text{He}} = 15 M_{\odot}$) which directly collapses into a BH with no mass ejection. For NSs, the ejected mass is calculated as: $M_{\text{ej}} = M_{\text{He}} - M_{\text{NS}}$, where M_{He} is the helium core mass ($M_{\text{He}} = [2.8 - 8] M_{\odot}$, see Tauris & van den Heuvel 2006), and $M_{\text{NS}} = 1.4 M_{\odot}$. For the BH case the models are:

- Model 1: high NK, $M_{\text{He}} = 8 M_{\odot}$, $M_{\text{ej}} = 0$;
- Model 2: low NK, $M_{\text{He}} = 8 M_{\odot}$, $M_{\text{ej}} = 0$;
- Model 3: high NK, $M_{\text{He}} = 8 M_{\odot}$, $M_{\text{ej}} = 4$;
- Model 4: low NK, $M_{\text{He}} = 15 M_{\odot}$, $M_{\text{ej}} = 0$.

For the NS case the models are:

- Model 5: high NK, M_{ej} uniform between $[1.4, 6.6] M_{\odot}$;
- Model 6: low NK, M_{ej} uniform between $[1.4, 6.6] M_{\odot}$.

For all the models, we simulate 3×10^7 binaries composed of the helium star (which core-collapses) and a companion star of $1 M_\odot$. The pre-SN orbital separation is uniformly drawn in the range $a_{\min} - 50 R_\odot$ with zero initial eccentricity, where a_{\min} is the minimal orbital separation such that either one of the two components fills its Roche lobe. We calculate the effect of the compact object formation on the orbital properties and on the kinematics of the binary (for more details on the method, see Repetto & Nelemans 2015). In particular, the effect of the mass ejection together with the NK impart a peculiar velocity to the binary:

$$V_{\text{pec}} = \sqrt{\left(\frac{M_{\text{BH}}}{M'}\right)^2 V_{\text{NK}}^2 + V_{\text{MLK}}^2} - 2 \frac{M_{\text{BH}}}{M'} V_{\text{NK},x} V_{\text{MLK}}, \quad (2)$$

where M' is the total mass of the binary after the SN, V_{NK} is the magnitude of the NK, $V_{\text{NK},x}$ its component along the orbital speed of the BH progenitor, and V_{MLK} is the *mass-loss kick*:

$$V_{\text{MLK}} = \frac{M_{\text{ej}}}{M'} \frac{M_\star}{M} \sqrt{\frac{GM}{a}}, \quad (3)$$

the recoil the binary gets because of the instantaneous mass ejection M_{ej} (M is the initial mass of the binary; M_\star is the mass of the companion; a is the initial orbital separation). We follow the evolution of the binaries under the coupling between tides and magnetic braking using the method developed in Repetto & Nelemans (2014), and select those systems that start mass transfer (MT), i.e. become X-ray sources, while the donor is on the main sequence.

We choose the radial distribution of the binaries to follow the surface density of stars in the thin disc: $\Sigma(R) \sim \Sigma_0 \exp(-R/R_d)$, with $R_d \sim 2.6$ kpc (McMillan 2011; Bovy et al. 2012), and with a maximum distance from the Galactic Centre of $R_{\max} = 10$ kpc. Concerning the height above the plane, we model it as an exponential with scale height h equal to the scale height of the thin disc ($h = 0.167$ kpc; Binney & Tremaine 2008). This is a conservative choice for the scale height, being the scale height of massive stars in the disc typically smaller ($h \sim 30$ pc; see Table 4 in Urquhart et al. 2014). We assume that the stars follow the Galactic rotation, with no additional component. Various mechanisms can heat up the stars in the disc, increasing their dispersion velocity, such as encounters with spiral density waves, giant molecular clouds, and various other forms of stochastic heating (Mihalas & Binney 1981; Sellwood & Preto 2002; Rocha-Pinto et al. 2004; Aumer et al. 2016). Rocha-Pinto et al. 2004, using a large sample of late-type dwarfs in the Milky Way disc, measured a dispersion in the three velocity-components of $\sigma_u \approx 50$ km/s, $\sigma_v \approx 30$ km/s, $\sigma_w \approx 20$ km/s at $t \approx 5 \times 10^9$ Gyr (see also Holmberg et al. 2009). We neglect this influence, as we expect that for low-mass stars hosted in (massive) binaries these velocity would be significantly lower.

We integrate the orbit of the binaries for 5 Gyr using the MWPotential2014 potential from Bovy (2015), which is a realistic model for the Milky Way potential. We record the position along the orbit every 5 Myr after 1 Gyr.

3.1 Observational samples

3.1.1 Black Hole X-ray Binaries

Using the catalogue of Corral-Santana et al. (2016), we classify the systems into three main groups:

- (i) short-period, dynamically confirmed BH-XRBs (9 systems);
- (ii) short-period, dynamically confirmed BH-XRBs + short-period BH candidates (15 systems);

Table 2. Galactic position of the three classes of BH-XRBs; R is the distance from the Galactic centre, $|z|$ is the absolute value of the height above the plane. In parenthesis we put the uncertainty on the measurements. See Corral-Santana et al. (2016) for the references for the distance measurements.

Name	R (kpc)	$ z $ (kpc)
short-period confirmed		
XTE J1118+480	8.74 (0.1)	1.52 (0.2)
GRO J0422+32	10.38 (0.65)	0.51 (1.15)
GRS 1009-45	8.49 (0.25)	0.62 (0.1)
1A 0620-00	8.93 (0.08)	0.12 (0.01)
GS 2000+251	7.21 (0.3)	0.14 (0.08)
Nova Mus 91	7.63 (0.2)	0.72 (0.1)
H 1705-250	0.53 (2.9)	1.35 (0.85)
XTE J1650-500	5.71 (1.35)	0.15 (0.075)
XTE J1859+226	10.03 (3.05)	1.87 (0.65)
long-period confirmed		
XTE J1550-564	4.96 (0.15)	0.14 (0.05)
GRS 1915+105	6.62 (0.99)	0.03 (0.008)
GS 2023+338 (V404 Cyg)	7.65 (0.001)	0.09 (0.005)
short-period candidates		
MAXI J1836-194	2.08 (1.15)	0.65 (0.25)
MAXI J1659-152	0.82 (1.55)	2.45 (1.05)
XTE J1752-223	2.15 (1.55)	0.22 (0.1)
SWIFT J1753.5-0127	3.64 (0.65)	1.27 (0.45)
4U 1755-338	1.56 (1.8)	0.55 (0.25)
GRS 1716-249	5.62 (0.4)	0.29 (0.05)

(iii) short- and long-period, dynamically confirmed BH-XRBs (12 systems),

which we list in Table 2, along with their Galactic position (R, z) derived from their sky-position and distance. Dynamically-confirmed BHs are those for which a dynamical measurement of the BH mass is available (see e.g. Casares & Jonker 2014).

The observed BH-XRBs are both long ($P_{\text{orb}} > 1$ day) and short orbital period ($P_{\text{orb}} \lesssim 1$ day), thereby originating from different evolutionary paths. Hence, in order to compare the observed systems with the simulated binaries, we need to produce two separate synthetic population of binaries, one population with short-period and one population with long-period, to which we compare the observed binaries according to their type. For the short-period binaries, we follow the binary evolution of simulated binaries using the method we explained in Section 3. For the long period ones, which are driven by the nuclear evolution of the donor, we model them assuming the post supernova orbital separation to be such that $a_{\text{circ}} = a_{\text{postSN}}(1 - e^2) \leq 20 R_\odot$, where a_{circ} is the circularised orbital separation and e is the eccentricity in the post-SN configuration. This assumption is based on the fact that long-period binaries evolve to longer and longer period during the MT phase, hence: $a_{\text{circ}} \approx a_{\text{MT},0} < a_{\text{MT},\text{obs}}$, where $a_{\text{MT},0}$ is the orbital separation at the onset of MT, and $a_{\text{MT},\text{obs}}$ is the observed orbital separation. The assumptions on the compact object formation are the same as for the short-period binaries, as well as the masses of the binary components. Since our simulated binaries have a companion mass of $1 M_\odot$, we exclude from the observed sample those binaries with a companion mass: $\gg 1 M_\odot$ (GRO J1655-40, 4U 1543-475, and SAX J1819.3-2525).

We account for a possible observational bias on the dynamically-confirmed BH-XRBs. In order to get a dynamical

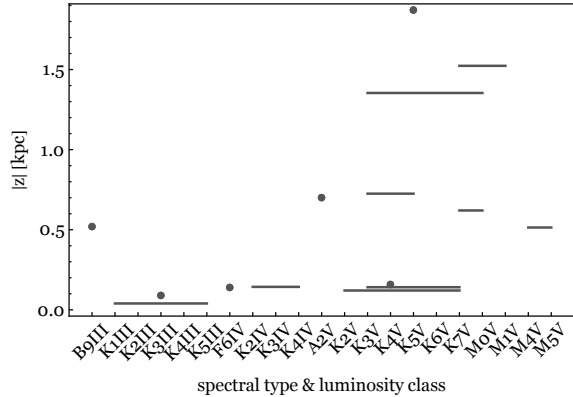


Figure 8. The height above the Galactic plane $|z|$ and the spectral type and luminosity class of the 15 dynamically-confirmed BH-XRBs. When the spectral type of the donor star in the system is not univocally identified, we indicate the range of possible types.

measurement of the BH mass, hence fully confirming the nature of the source, high signal-to-noise optical spectra are required; this might be prevented in regions of high extinctions, i.e. in and close to the Galactic plane. We then remove from our simulated populations those binaries which are located at $z \leq 0.1$ kpc. We note that the lowest z in the sample of short-period dynamically confirmed BH binaries is for 1A 0620-00 ($z \approx -0.12$ kpc; see Table 2). For the long-period binaries, we exclude from the study the sources GRS 1915+105 (donor spectral type: K1/5 III) and V404 Cyg (donor spectral type: K0 IV), which are located at $z \approx -0.03$ kpc and $z \approx -0.09$ kpc respectively (see Table 2). These two systems do have a dynamical measurement of the BH mass (see Casares & Jonker 2014). In Figure 8 we plot the absolute value of the height z versus the spectral type and luminosity class of the 15 ¶ dynamically-confirmed BH-XRBs (the spectral types are from Corral-Santana et al. 2016). At small z , stars have an earlier spectral type and/or are giants or sub-giants. Whereas MS/dwarf stars tend to be seen at larger distances above the plane.

The only long-period binary in our sample, after removing those sources close to the Galactic plane, is XTE J1550-564, which has a current orbital separation of $12 R_{\odot}$, consistent with our assumption on a_{circ} .

3.1.2 Neutron Star X-ray Binaries

The Galactic population of NS-XRBs consists of more than 30 objects (see Jonker & Nelemans 2004 and references therein). For our study, we select the 10 ones with a short-orbital period ($P_{\text{orb}} < 1$ day; see Table 2 in Jonker & Nelemans 2004). The identification of a NS-XRB typically occurs via the detection of X-ray bursts which ignite on the surface of the NS. Therefore, unlike for BHs, there are potentially no biases against the identification of such systems.

¶ 12 systems from Table 2 to which we add the three BH-XRBs with an intermediate-mass companion.

4 Results of the Binary Population Synthesis

4.1 The expected vertical distribution of BH- and NS-XRBs

The scale height of BH- and NS-XRBs is a proxy of the effect of different compact object formation mechanisms on to the Galactic distribution of the binaries. We quantify the scale height of the binaries as the rms of their height z as a function of R for all points. To plot the results, we bin the systems into 1 kpc-wide bins in the R -direction. We show the results in Figure 9 for the six models. The monotonic rise of z_{rms} is expected, since the Galactic potential becomes weaker further away from the Galactic centre, and the binary moves further up for the same initial velocity. It is interesting to note that if BHs and NSs receive the same NK, they would still show a different scale height, with NSs reaching larger distances from the Galactic plane (compare black solid line with grey solid line, and black dashed line with grey dashed line). This is due to the fact that for the same linear momentum, a binary with a larger mass receives a lower V_{pec} (as is shown in Figure 10). If the progenitor of the BH ejects mass at core-collapse as in Model 3 (see black dashed-dotted line in Figure 9), it will move further out from the plane than when no mass is ejected, since the mass ejection adds an extra contribution to V_{pec} . Furthermore, V_{pec} does not depend on the mass of the BH when no mass is ejected at BH formation (black dashed and black dotted lines in Figure 9), since it scales as

$$V_{\text{pec}} = \sqrt{\left(\frac{M_{\text{BH}}}{M_{\text{BH}} + M_2}\right)^2 V_{\text{NK}}^2} \sim V_{\text{NK}}, \text{ for low-mass companion stars (see equation 2).}$$

In Figure 10 we also show as arrows the lower limits on the peculiar velocity at birth of the 9 BH-XRBs we studied in Section 2.2. It is clear that a high-NK distribution (darker-grey solid line) more easily accounts for the higher-velocity systems, as 4 systems lie in or beyond the high-velocity tail of the distribution corresponding to the low-NK model.

Jonker & Nelemans (2004) found a similar z_{rms} between NS- and BH-XRBs and deduced that BHs should receive NKs too, unless differences in the binary evolution and observational biases were strong. We confirm that accounting for binary evolution does not strongly change the Galactic distributions of BH- and NS-XRBs. However, the scale height does strongly depend on the position in the disc.

We compute the z_{rms} of the observed BH-XRBs, both of the whole sample and of the dynamically-confirmed systems only. We find a rms of $\approx 0.98 \pm 0.10$ kpc and $\approx 0.86 \pm 0.10$ kpc respectively. For the short-period NS systems, we calculate a z_{rms} of 1.24 ± 0.06 kpc, when excluding the source XTE J2123-058 since its velocity is consistent with being a halo source, as Jonker & Nelemans (2004) noted. The error on these z_{rms} -values accounts for the uncertainty on the distance to the sources. In Figure 11 we show the Galactic distribution of NS and BH systems (the lines account for the uncertainty in the distance to the source). The result that NS systems should have a larger scale height than BH systems is consistent with what the observed populations show.

4.2 The influence of the orbital separation distribution of the binary progenitors

In the models we used in Section 3, the orbit of the binary progenitors of BH- and NS-XRBs was chosen to be uniformly distributed in the range $[a_{\text{min}}, 50] R_{\odot}$. It could be that this choice biases our results towards certain values for V_{pec} . To test this, we check how the distribution of the initial orbital separation of the binaries (i.e. prior to the formation of the compact object) varies with the magnitude

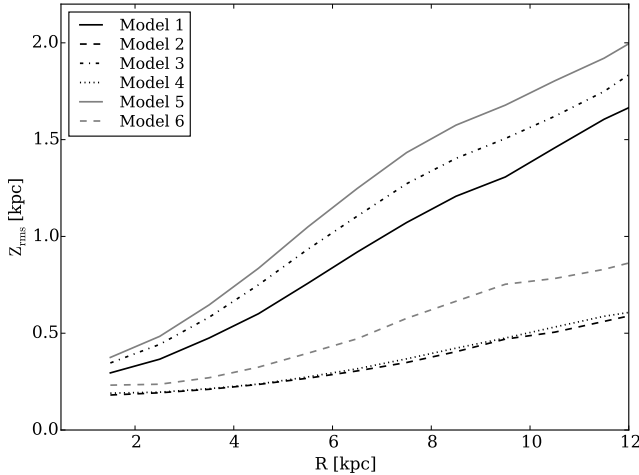


Figure 9. Root-mean-square of the height z above the Galactic plane of simulated BH- and NS-XRBs for the different models used.

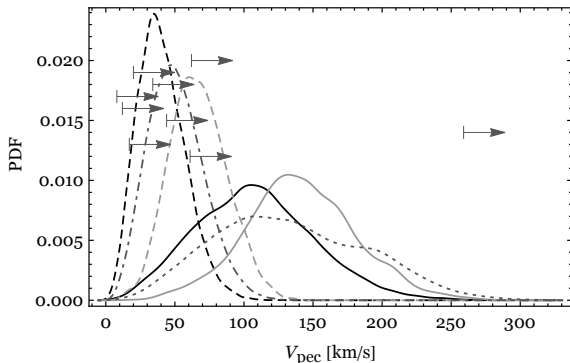


Figure 10. Distribution of the peculiar velocity V_{pec} (after the formation of the compact object) of BH-XRBs in Model 1 (black solid line) and Model 2 (black dashed line), and of NS-XRBs in Model 5 (grey solid line) and Model 6 (grey dashed line). The dotted and dotted-dashed dark-grey lines are variations of Model 1 (see Section 5 for details). The arrows represent the lower limits on the peculiar velocity at birth for the 9 short-period BH-XRBs using the potential from Bovy (2015).

of the NK and of V_{pec} . From Figure 12, it is clear that the majority of the initial orbital separations are constrained to lie within a small range ($a_{\text{preSN}} \lesssim 10 R_{\odot}$) both for NS and BH systems, and both for high and low NKs. Furthermore, there is no clear trend of V_{pec} with respect to a_{preSN} . We hence conclude that it is unlikely that the peculiar velocities V_{pec} would be very much influenced if the pre-SN orbits had a distribution different from the uniform one we use in our study, or if they were drawn from a smaller range.

4.3 Comparison with observations: BH-XRBs

We now turn to the comparison of the different models with the observed BH-XRBs. In order to compare the simulations with the observed systems, we note that every subgroup of BH binaries of Table 2 gives rise to a certain 2D distribution in R and z . One way of proceeding would be to compare the 2D simulated distribution with the 2D observed one. We compare the data with the simulated populations dividing the Galaxy into 1 kpc-wide bins along the R -direction. This allows to account for the fact that the Galactic potential is a strong function of the position in the disk, as we

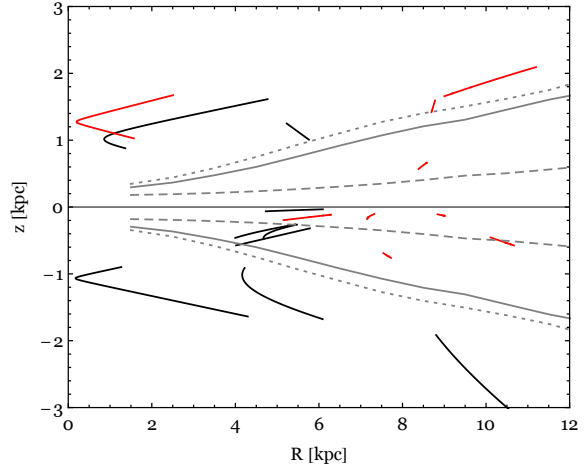


Figure 11. Galactic distribution of BH-XRBs (red lines) and NS-XRBs (black lines). R is the distance from the Galactic center projected on to the plane, and z is the height above the plane. One NS-XRB falls off the figure: XTE J2123-058. For each source, the line accounts for the uncertainty on the distance. We also show the results from the population study in terms of z_{rms} as a function of R : Model 1 (grey lines), Model 2 (grey-dashed lines), Model 3 (grey-dotted lines).

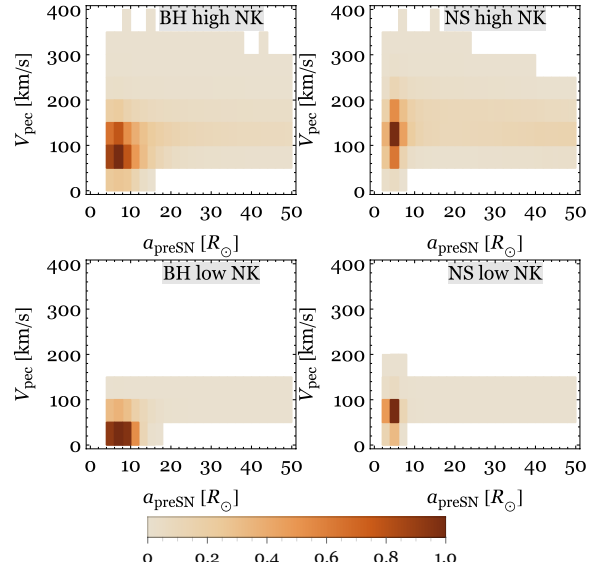


Figure 12. Density plots which result from our population synthesis models showing the allowed parameter space for the peculiar velocity at birth V_{pec} and the orbital separation a_{preSN} of BH- and NS-XRBs prior to the formation of the compact object. Each panel corresponds to different assumptions on the NK. The fraction of systems in each 2-dimensional bin is shown; darker colours correspond to a larger fraction of systems.

showed in Section 2.2. For every R -bin, we compute the cumulative distribution function (CDF) of the height z above the Galactic plane based on the population synthesis results within Model 1 and Model 2 (see as an example black and grey lines in Figure 13, for the bin: $R = [8, 9]$ kpc). Then we calculate where in the cumulative distribution the observed systems lie (see as an example the intersection between the blue vertical lines and the CDFs in Figure 13). In such a way, we obtain a list of percentiles. If the model is correct, we expect these percentiles to be drawn from the uniform distribution. We note that we have removed from our comparison

those sources located in the bulge of the Galaxy (i.e. H 1705-250 and MAXI J1659-152), which could have had a different origin rather than having formed in the plane (see Section 2.2). We plot the cumulative distribution of these percentiles in Figures 14 (short-period confirmed BH-XRBs), 15 (short-period confirmed + candidates), and 16 (whole sample). In the figures, the solid lines correspond to Model 1 and the dashed lines correspond to Model 2. We also consider a model which consists of a superposition of Model 1 and Model 2 in equal parts (see thin solid in Figure 14, in the case of the short-period confirmed BH-XRBs). The model which fits best is the one which comes closer to the diagonal line (that represents the cumulative of a uniform distribution). In all three cases, a high NK distribution is the most preferable one.

We perform a Kolmogorov-Smirnov (KS) test to measure how close is the distribution of percentiles to the diagonal line of Figures 14, 15, 16. We summarise the D -values and their corresponding probabilities in Table 3 for every subgroups of BH-XRBs. For each of the sub-groups the high-NK model fits the data best, although in the group with confirmed BHs only, the low-NK is also consistent with the data. For the confirmed+candidate short-period systems as well as for the whole sample, the low-NK model is inconsistent. Interestingly, the model in which the BHs receive both low and high NKs, fits the data best for the confirmed systems.

In these results, we have excluded all the systems in the plane (both observed and simulated). An accurate modelling of the obscured systems would require a model for the Galactic extinction in and out of the plane combined with a model for the optical/NIR magnitudes of BH-XRBs in their quiescent state. As a first step, we simplistically model the observational effects near the Galactic plane including a certain fraction of those simulated points which end up in the Galactic disc (at $z \leq 1$ kpc): either $f_{\text{disc}} = 0.1$, or 0.5, or 0.9. We compare the Galactic distribution of these simulated binaries with the distribution of the whole sample of binaries, including this time the obscured sources GRS 1915+105 and V404 Cyg as well. The results are presented in Figure 17 and Table 3. Also when including the obscured systems, the high-kick model is the most successful in reproducing the observed binaries.

4.3.1 Effect of the distance uncertainty

The distance d to a BH-XRB is typically estimated by measuring the apparent magnitude of the companion star in a certain colour band, and computing its absolute magnitude. Once an estimate of the reddening towards the source is known and the spectral type of the donor star is clearly identified, the distance can be calculated. In the best case scenario, one would have the apparent magnitude of the source in different bands, and then would compute the scatter between the derived distances as estimate of the distance uncertainty. We expect such uncertainties to follow a Gaussian distribution. However, in case a range of spectral types is equally probable, we expect the errors on the distance to be distributed more uniformly. To investigate the influence of the uncertainty in the distance, and since for most of the literature there is no easy way of determining the type of error distribution, we randomly generate 100 values for the distance to each BH-XRB, either distributed as a Gaussian (with σ equal to the distance uncertainty δ) or as a uniform distribution in the range $(d - \delta, d + \delta)$. Such errors can cause a binary to move from one R -bin to the adjacent one, affecting the percentile values. However, we find that there is no systematic shift that would make low NKs fit best the observed data, δ being smaller than the discrepancy between the two distributions.

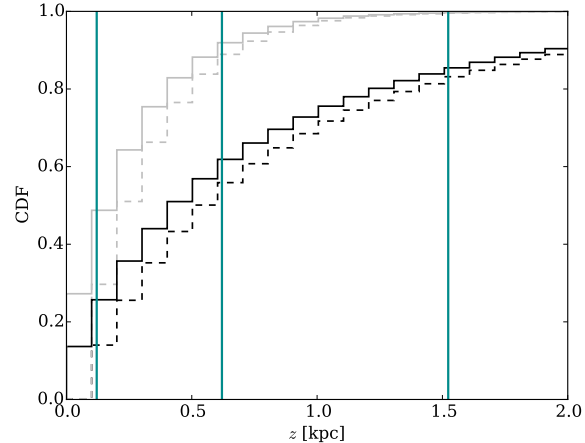


Figure 13. The cumulative distribution for $|z|$ for Model 1 (black lines) and Model 2 (grey lines), in the bin $R = [8, 9]$ kpc. Solid lines correspond to the whole sample of simulated binaries; dashed lines correspond to the remaining part of the sample after the exclusion of systems close to the Galactic plane, i.e. $z \leq 0.1$ kpc. The blue vertical lines represent the observed $|z|$ of 3 BH-XRBs (from left to right: 1A 0620-00; GRS 1009-45; XTE J1118+480).

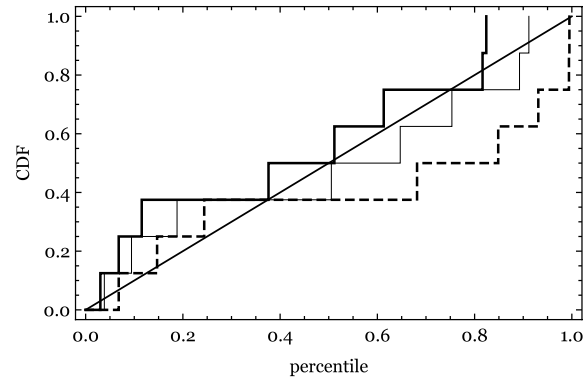


Figure 14. Cumulative distribution of the percentiles associated with short-period dynamically-confirmed BH-XRBs in Model 1 (solid line) and Model 2 (dashed line). The thin solid line is a blend of Model 1 and 2 (50 – 50%). The model which fits best the observed data is the one closer to the diagonal line.

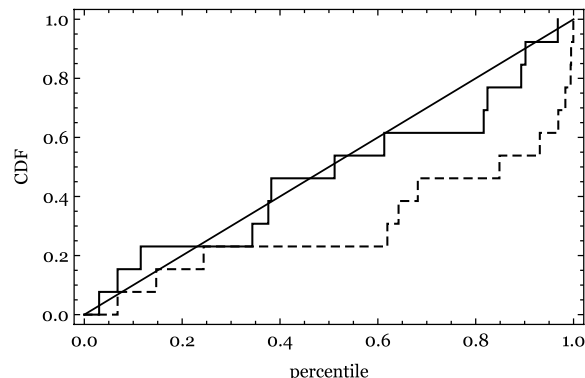


Figure 15. Cumulative distribution of the percentiles associated with short-period dynamically-confirmed and candidate BH-XRBs in Model 1 (solid line) and Model 2 (dashed line). The model which fits best the observed data is the one closer to the diagonal line.

Table 3. D-values of the KS-test for different systems and in the different models: Model 1 (i.e. high NK), Model 2 (i.e. low NK), and a model made of a superposition of the high- and low-NK in equal parts.

Subgroup	High NK D (P)	Low NK D (P)	50-50 D(P)	N	Fig.
BH-XRBs, short P, confirmed	0.26 (0.57)	0.34 (0.24)	0.19 (0.92)	8	14
BH-XRBs, short P, confirmed+candidates	0.20 (0.61)	0.39 (0.03)	0.28 (0.22)	13	15
BH-XRBs, whole sample	0.17 (0.77)	0.36 (0.04)	0.26 (0.24)	14	16
BH-XRBs, whole sample, $f_{\text{disc}} = 0.1$	0.20 (0.46)	0.29 (0.12)	0.19 (0.54)	16	17
BH-XRBs, whole sample, $f_{\text{disc}} = 0.5$	0.13 (0.96)	0.33 (0.04)	0.20 (0.47)	16	17
BH-XRBs, whole sample, $f_{\text{disc}} = 0.9$	0.14 (0.91)	0.37 (0.01)	0.22 (0.37)	16	17
NS-XRBs	0.39 (0.06)	0.63 (0.00)	-	10	18

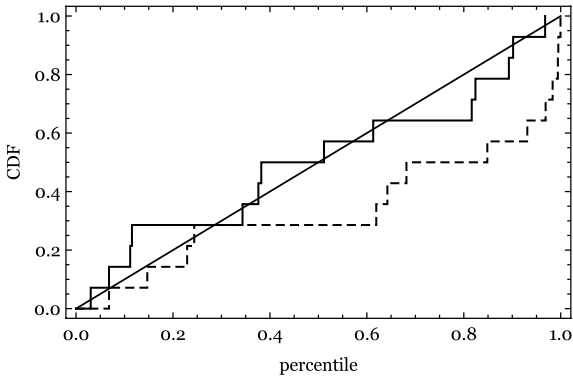


Figure 16. Cumulative distribution of the percentiles associated with the whole sample of BH-XRBs in Model 1 (solid line) and Model 2 (dashed line). The model which fits best the observed data is the one closer to the diagonal line.

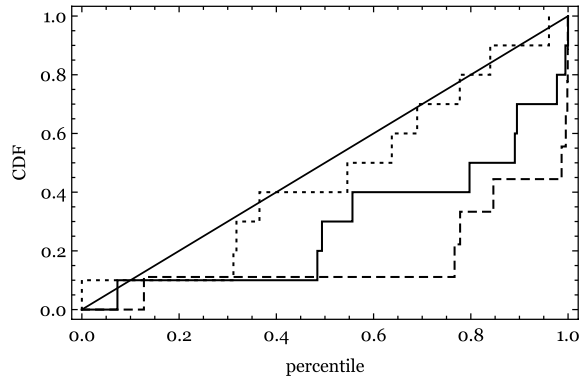


Figure 18. Cumulative distribution of the percentiles associated with short-period NS-XRBs in Model 5 (solid line) and Model 6 (dashed line). Dotted line is when the NK is drawn from the Hobbs distribution. The model which fits best the observed data is the one closer to the diagonal line.

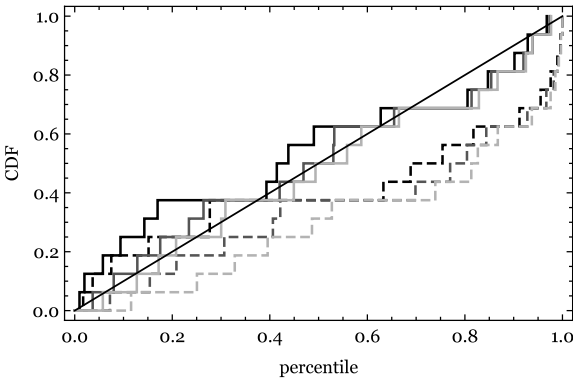


Figure 17. Cumulative distribution of the percentiles associated with the whole sample of BH-XRBs in Model 1 (solid lines) and Model 2 (dashed lines) when assuming a different fraction of systems in the Galactic plane: $f_{\text{disc}} = 0.1$ (black lines), 0.5 (darker grey lines), or 0.9 (lighter grey lines). The model which fits best the observed data is the one closer to the diagonal line.

4.4 Comparison with observations: NS-XRBs

We compare the observed z distribution of NS systems with the distribution of the two simulated population of NS-XRBs in the context of Model 5 and Model 6. We perform the comparison in the same way we did for BH-systems in Section 4.3. From Figure 18 we see that none of the distributions (solid and dashed lines) fits the data. Our goal is not to calibrate the NS NK distribution from

the NS-XRB population, nor from a population model of radio pulsars (cf. Hartman et al. 1997). Nevertheless, we can note that the observed population of NS-XRBs seems to be consistent with NKs larger than ≈ 100 km/s. This is in line with the catalogue of pulsar proper motions by Hobbs et al. 2005, who inferred a mean pulsar birth velocity of ≈ 400 km/s. However, the derivation of pulsar velocities from the measured proper motions has to be taken with caution, because of the possible uncertainties in the proper motion measurements as well as in the distance measurements. More in general, underestimating proper motion measurement errors can lead to an overestimate of pulsar velocities, as noted by Hartman (1997). The distance to a pulsar is typically estimated through parallax. Igoshev et al. (2016) showed that a more proper Bayesian approach to calculate the distance probability function from a single parallax measurement has to be used. Such method has not been applied yet to the whole population of pulsars.

We show the results of the KS-test for NS systems in Table 3: both models have large D -values.

For an illustrative purpose, we also compare the observed population of NS-XRBs to a simulated one in which the NK is drawn from a Maxwellian distribution with $\sigma = 265$ km/s (Hobbs et al. 2005). The results of the KS test favours this distribution: $(D, p)_{\text{Hobbs}} = (0.21, 0.72)$; see dotted line in Figure 18.

We note that we did not include the long-period NS-XRBs to our study as in the sample of NS-XRBs from Jonker & Nelemans 2004 that we are using, there is only one long-period system with a low-mass companion, Cygnus X-2.

5 Discussion

(i) In our models of Section 3, we have assumed an ejected mass at BH formation of 0 or $4 M_{\odot}$. Taking $M_{\text{ej}} = 8 M_{\odot}$ would not greatly affect the scale height of the binaries in the case of a high NK distribution, since the typical peculiar velocities are comparable to the case when $4 M_{\odot}$ are ejected (see dotted line in Figure 10). This is due to the fact that a high ejected-mass is compatible only with the lower-velocity tail of the NK distribution in order for the binary to stay bound. In the case of a low NK distribution, the higher ejected-mass has a greater effect on the average peculiar velocity (see dashed-dotted line in Figure 10). However, the NS systems velocities are still larger. In order for BH systems to have the same peculiar velocity as NS systems, we would need that $V_{\text{MLK,BH}} = V_{\text{MLK,NS}} + (1/2) \times V_{\text{NK}}$, which follows from the expression for V_{pec} (equation 2), imposing that $V_{\text{pec,BH}} = V_{\text{pec,NS}}$ and assuming that $V_{\text{NK,x}} = V_{\text{NK}}$. This would constraint M_{ej} to be much larger than what is allowed for the binary to stay bound.

(ii) In the modelling of the progenitors of BH- and NS-XRBs, we have assumed a flat distribution of the initial orbital separation in the range $[a_{\text{min}}, 50] R_{\odot}$ (Section 3). With this choice, we are including all possible pre-SN orbital separations. In Repetto & Nelemans (2015) we verified that larger separations do not contribute to the final separation of the binary (see their Figure 13). This is due to the fact that the strength of the coupling between tides and magnetic braking, which is responsible for the shrinking of a binary to short orbital periods, decreases strongly with larger orbital separations. For long-period BH-XRBs, this choice is also acceptable, as none of the observed binaries in our sample have an orbital separation larger than $50 R_{\odot}$. There could be of course cases in which the orbit in the post-SN phase is highly eccentric and very wide, but these cases would contribute only to a minority of the systems. More importantly, we have found that the NK distribution does not in fact depend on the pre-SN orbital period (see Figure 12, where there is no trend of the orbital separation depending on the NK). We can also compare the circularised orbital period distribution after the SN in our models, $P_{\text{orb,circ}}$, with the one in Pfahl et al. 2003, who did detailed evolutionary calculations of NS-LMXBs. In our models, $P_{\text{orb,circ}}$ ranges from ≈ 0.15 days to ≈ 12 days, which is compatible with the range shown by Pfahl et al. 2003 in their Figure 1.

(iii) We have assumed that the companion of BHs and NSs are stars with an initial mass of $1 M_{\odot}$. Pfahl et al. (2003) argued that the majority of LMXBs have likely originated from binaries with an intermediate mass companion ($\approx 2-3 M_{\odot}$). We have checked how our results would be affected when taking a companion of initial mass: $3 M_{\odot}$. The peculiar velocity right after the BH formation (see Figure 10) would decrease due to the larger binary mass: by a factor of ≈ 0.6 on average. This implies that the NK would need to be even larger in order for the simulated systems to match the observed ones.

(iv) The two Maxwellian distributions used in Section 3 do not correspond to the real physical distributions, but rather are representative of two complementary distributions, one generating large kicks, the other generating low kicks. The choice of two distributions peaked at two different velocities serves the purpose of analysing how close in magnitude are the velocities received by BHs with respect to the velocities received by NSs. The NK distribution of NSs can be estimated via proper motion studies of pulsars. The pulsar birth speed distribution has been estimated as a Maxwellian distribution with $\sigma = 265$ km/s by Hobbs et al. 2005; however, one should bear in mind the caveats discussed in Sec-

tion 4.4. For BHs, the number of sources with measured 3D space velocity (5; see Miller-Jones 2014) is not sufficient to allow for a calibration of their NK distribution.

(v) When comparing the observed BH-XRBs with the synthetic BH-XRBs which result from our population synthesis, we found that the population in which BHs receive high NKs best fit the observed data. This conclusion gains strength when including in the comparison between observations and simulated population the sources located in the bulge of the Galaxy (i.e. H 1705-250 and MAXI J1659-152). In this case, the KS-values for the short-period confirmed BH-XRB sample are: $(D, p)_{\text{highNK}} = (0.22, 0.74)$, $(D, p)_{\text{lowNK}} = (0.40, 0.08)$, and for the short-period confirmed + candidates BH-XRB sample are: $(D, p)_{\text{highNK}} = (0.28, 0.15)$, $(D, p)_{\text{lowNK}} = (0.46, 0.00)$.

(vi) We did not include the long-period NS-XRBs in our study. We can still investigate how much long- and short-period NS-XRBs differ when it comes to the peculiar velocity after the SN, and hence how they differ in terms of the scale height above the Galactic plane. We build a population of binaries which evolve into long-period NS-XRBs along the lines of the computational method used for long-period BH-XRBs (see Section 3). We find that the long-period systems have slightly lower peculiar velocities, which results in a slightly lower scale height (by a factor of ≈ 0.8 , for every radial distance). This is due to the fact that the binary, having lower binding energy, can only survive lower kicks.

(vii) As it was mentioned in the introduction, there is evidence for some NSs receiving low kicks at birth: NSs residing in double-NS systems (Wong et al. 2010; Beniamini & Piran 2016; Chruslinska et al. 2016) and NSs hosted in a subset of high-mass X-ray binaries (HMXBs; Pfahl et al. 2002). It was suggested that electron-capture SNe are too fast for large asymmetries to develop, resulting in a modest kick, of a few 10 km/s at maximum. Such kicks are of the order of the low natal kick model we took in our binary population synthesis of Section 3 through which we found (Section 4.4) that high-kick models best fit the Galactic distribution of NS-LMXBs: i.e. we did not find any evidence for NSs born in an electron-capture SN. This might be due to a different evolutionary path for the progenitors of NS-LMXBs. Several studies have investigated the type of SN event (either a standard collapse of the iron core or an electron capture SN) as a function of the evolutionary state of the helium star progenitor of the NS as well as the characteristics of the binary orbit. Tauris et al. 2015 performed detailed evolutionary sequences of binaries hosting an NS and a helium star. They found that helium stars with an initial mass of $2.6 - 2.95 M_{\odot}$ could be stripped of a significant fraction of their mass through case BB mass transfer towards an NS companion when the helium star expands as a giant. The low-mass core would then form an NS via electron-capture SN, provided the initial orbital period is sufficiently wide. Shorter orbital period would instead result in a white dwarf (WD). We can extrapolate this finding to the short-period systems formed by an NS and a low-mass companion studied in our work. However, we must bear in mind that the stripping effect is less understood for a giant helium star experiencing mass transfer to a low-mass main-sequence star, as indeed mentioned by Tauris et al. 2015. Thus we conclude that, heretofore, there is no strong theoretical support for a preference for electron-capture SN in the progenitors of NS-LMXBs. We also wish to note that the study by Kalogera & Webbink 1998 highlighted the impossibility of forming short-period (less than one day) NS-LMXBs without large natal kicks at birth (where for large they chose a Maxwellian distribution with an average kick of 300 km/s).

5.1 A note on our KS-test

In assessing the quality of the fit of our simulations, we used the classical application of the KS-test. In order to test its validity and determine the *power* of the test in distinguishing the two hypothesis we draw samples of various sizes from the simulated populations, and we calculate the D -value distribution of each of these samples, according to the rules described in Section 4.3. We find that the probabilities follow the classical KS test (as expected) to an accuracy (5%) that is comparable to the Poisson noise in our simulations ($\approx 3\%$). More interesting is the measurement of how often we obtain D -values smaller than the ones we measured for our observed samples when *testing the wrong hypothesis* - i.e. when using a sample drawn from the high (low) NK synthetic population and testing the low (high) NK hypothesis (also known as false negative rate). For the BH case, we find D -values smaller than the ones in Table 3 in less than $\beta \approx 10\%$ of the cases, for the high NK hypothesis, and in more than $\beta \approx 30\%$ for the low NK hypothesis. A particularly interesting fact is that $\beta = 0.015$ for short-period confirmed + candidate BH-XRBs. If we accept the $\alpha = 3\%$ confidence level and use the standard 4-to-1 weighting (i.e. $4\alpha = \beta$), the test we developed has enough power to distinguish between the high- and low-NK hypothesis in this case, and that the high-NK hypothesis is clearly preferable. This is a *non*-expected result given the small number of object, and it can potentially dissolve if some of the BH candidates turn out to be NS-XRBs. To calculate what is the optimal number of observed systems to decrease such rate β , we draw samples of various sizes from the population synthesis results of Model 1 and we test the low-NK hypothesis, and vice-versa. To decrease this rate to the level that in 95% of cases we obtain $\beta < 1\%$, we find that it is necessary to increase the size of the observed sample to ≈ 40 systems, both in the BH and NS case.

6 Conclusions

In this work we performed a binary population synthesis study of BH- and NS-XRBs, tracing their binary evolution from the moment of compact object formation until the observed phase of mass transfer, and integrated their orbits in the Galaxy. The main goal was to investigate whether different assumptions on compact object formation manifest themselves in the Galactic distribution of the binaries. We found that these assumptions do affect the scale height of the binaries, which we quantified through their z_{rms} . In particular, we found that if BHs and NSs receive the same NK at birth, NSs would still have a larger scale height above the Galactic plane, due to the fact that their systemic velocities acquired when the compact object is formed are typically larger, their total binary mass being smaller. The larger scale height of NS-XRBs with respect to BH-XRBs is clearly seen also in the observed populations. We also found a clear trend for both populations of increasing scale height for larger Galactocentric radii, which should manifest itself, but which is not clearly observed in the current populations (see Figure 11).

The main outcome of this study is that when analysing the z -distribution of the observed BH systems as a function of R , the simulated population in which at least some BHs receive a (relatively) high NK (~ 100 km/s) fits the data best. This is in agreement with previous findings by Repetto et al. (2012), who compared the observed and simulated populations of BH-XRBs only in the z -direction, whereas we compare the 2D distributions, accounting for how the binaries are distributed along the R -direction as

well. Furthermore, we increased the sample of sources adding 6 BH candidates, updated their distances according to the recently published BH catalogue of Corral-Santana et al. (2016), and followed the binary evolution of the binaries in a detailed way (accounting in particular for magnetic braking and tides).

In this work we also checked numerically the validity of a simple one-dimensional analytical estimate for the peculiar velocity at birth of BH-XRBs which we used in our previous works Repetto et al. (2012) and Repetto & Nelemans (2015). We found that this estimate is less reliable for some gravitational potentials for sources in the bulge of the Galaxy, i.e at $R \leq 1$ kpc. This was also shown by Mandel (2016), who studied the kinematics of H 1705-250, a BH-XRB close to the Galactic bulge. However, the estimate is robust for systems at Galactocentric radii larger than 1 kpc. Repetto & Nelemans (2015) followed the binary evolution of seven short-period BH-XRBs and estimated their minimal peculiar velocity at birth, to conclude that two out of the seven sources were consistent with a high (or relatively high) NK at birth. This conclusion remains valid even in view of the current analysis.

Jonker & Nelemans (2004) found that the rms-value of the distance to the Galactic plane for BH-XRBs was similar to that of NS-XRBs. This was suggestive for BHs receiving a kick-velocity at formation. We revised the distances and updated the sample of BH-XRBs using the catalogue from Corral-Santana et al. (2016) and we found that NS systems have a larger scale height than BH systems, a trait which is also present in the simulated populations.

Finally, we found that the comparison of the data to our simulations is limited by the small number of observed BH-XRBs, and thus that more systems should be found to determine in more detail the NK that BHs receive. In this respect, the possible future discovery of new BH transients with Gaia (Maccarone 2014), and through dedicated surveys such as the Galactic Bulge Survey (Jonker et al. 2011), are promising.

7 Acknowledgments

SR is thankful to Jo Bovy for answering her questions concerning Galpy and for useful comments on the manuscript. SR wishes to warmly thank her office mates (Pim van Oirschot, Martha Irene Saladino, Laura Rossetto, Thomas Wevers) at Radboud University for their great moral support during the hectic times of finishing up her thesis. SR wishes to acknowledge Melvyn B. Davies with whom she started her research on black hole natal kicks. This research has made use of NASA's Astrophysics Data System.

REFERENCES

- Aumer M., Binney J., Schönrich R., 2016, MNRAS, 462, 1697
- Belczynski K., Kalogera V., Rasio F. A., Taam R. E., Zezas A., Bulik T., Maccarone T. J., Ivanova N., 2008, ApJS, 174, 223
- Belczynski K., Repetto S., Holz D. E., O'Shaughnessy R., Bulik T., Berti E., Fryer C., Dominik M., 2016, ApJ, 819, 108
- Beniamini P., Piran T., 2016, MNRAS, 456, 4089
- Binney J., Tremaine S., 2008, Galactic Dynamics: Second Edition. Princeton University Press
- Bovy J., 2015, ApJS, 216, 29
- Bovy J., Rix H.-W., Liu C., Hogg D. W., Beers T. C., Lee Y. S., 2012, ApJ, 753, 148
- Brandt N., Podsiadlowski P., 1995, MNRAS, 274, 461
- Burrows A., Dolence J. C., Murphy J. W., 2012, ApJ, 759, 5

Casares J., Jonker P. G., 2014, *Space Sci. Rev.*, 183, 223

Chruslinska M., Belczynski K., Bulik T., Gladysz W., 2016, ArXiv e-prints

Corral-Santana J. M., Casares J., Muñoz-Darias T., Bauer F. E., Martínez-Pais I. G., Russell D. M., 2016, *A&A*, 587, A61

De Lucia G., Fontanot F., Wilman D., Monaco P., 2011, *MNRAS*, 414, 1439

Dhawan V., Mirabel I. F., Ribó M., Rodrigues I., 2007, *ApJ*, 668, 430

Fragos T., Willems B., Kalogera V., Ivanova N., Rockefeller G., Fryer C. L., Young P. A., 2009, *ApJ*, 697, 1057

Fryer C., Kalogera V., 1997, *ApJ*, 489, 244

Fryer C. L., Kalogera V., 2001, *ApJ*, 554, 548

Fryer C. L., Warren M. S., 2002, , 574, L65

Gerhard O., 2015, in Points S., Kunder A., eds, *Fifty Years of Wide Field Studies in the Southern Hemisphere: Resolved Stellar Populations of the Galactic Bulge and Magellanic Clouds* Vol. 491 of *Astronomical Society of the Pacific Conference Series*, *Formation Models of the Galactic Bulge*. p. 169

Hansen B. M. S., Phinney E. S., 1997, *MNRAS*, 291, 569

Hartman J. W., 1997, *A&A*, 322, 127

Hartman J. W., Bhattacharya D., Wijers R., Verbunt F., 1997, *A&A*, 322, 477

Hobbs G., Lorimer D. R., Lyne A. G., Kramer M., 2005, *MNRAS*, 360, 974

Holmberg J., Nordström B., Andersen J., 2009, *A&A*, 501, 941

Igoshev A., Verbunt F., Cator E., 2016, *A&A*, 591, A123

Irrgang A., Wilcox B., Tucker E., Schiefelbein L., 2013, *A&A*, 549, A137

Irwin J. A., 2005, *ApJ*, 631, 511

Janka H.-T., 2012, *Annual Review of Nuclear and Particle Science*, 62, 407

Janka H.-T., 2016, ArXiv e-prints

Johnston H. M., 1996, in Wijers R. A. M. J., Davies M. B., Tout C. A., eds, *NATO Advanced Science Institutes (ASI) Series C* Vol. 477 of *NATO Advanced Science Institutes (ASI) Series C*, *An Observational Approach to Binary Population Synthesis*. p. 385

Johnston S., Manchester R. N., Lyne A. G., Bailes M., Kaspi V. M., Qiao G., D'Amico N., 1992, , 387, L37

Jonker P. G., Nelemans G., 2004, *MNRAS*, 354, 355

Jonker et al. P. G. e. a., 2011, *ApJS*, 194, 18

Kalogera V., Kolb U., King A. R., 1998, *ApJ*, 504, 967

Kalogera V., Webbink R. F., 1998, *ApJ*, 493, 351

Kaspi V. M., Johnston S., Bell J. F., Manchester R. N., Bailes M., Bessell M., Lyne A. G., D'Amico N., 1994, , 423, L43

Kolb U., Davies M. B., King A., Ritter H., 2000, *MNRAS*, 317, 438

Lyne A. G., Lorimer D. R., 1994, *Nature*, 369, 127

Maccarone T. J., 2014, *Space Sci. Rev.*, 183, 477

Mandel I., 2016, *MNRAS*, 456, 578

McMillan P. J., 2011, *MNRAS*, 414, 2446

Mihalas D., Binney J., 1981, *Galactic astronomy: Structure and kinematics /2nd edition/*

Miller-Jones J. C. A., 2014, *Publications of the Astronomical Society of Australia*, 31, e016

Miller-Jones J. C. A., Jonker P. G., Nelemans G., Portegies Zwart S., Dhawan V., Brisken W., Gallo E., Rupen M. P., 2009, *MNRAS*, 394, 1440

Mirabel I. F., Rodrigues I., 2003, *Science*, 300, 1119

Nelemans G., 2007, in St.-Louis N., Moffat A. F. J., eds, *Massive Stars in Interactive Binaries* Vol. 367 of *Astronomical Society of the Pacific Conference Series*, *What Can We Learn About Black-Hole Formation from Black-Hole X-ray Binaries?*. p. 533

Nelemans G., Tauris T. M., van den Heuvel E. P. J., 1999, *A&A*, 352, L87

Özel F., Psaltis D., Narayan R., McClintock J. E., 2010, *ApJ*, 725, 1918

Paczynski B., 1990, *ApJ*, 348, 485

Pfahl E., Rappaport S., Podsiadlowski P., 2003, *ApJ*, 597, 1036

Pfahl E., Rappaport S., Podsiadlowski P., Spruit H., 2002, *ApJ*, 574, 364

Podsiadlowski P., Langer N., Poelarends A. J. T., Rappaport S., Heger A., Pfahl E., 2004, *ApJ*, 612, 1044

Remillard R. A., Orosz J. A., McClintock J. E., Bailyn C. D., 1996, *ApJ*, 459, 226

Repetto S., Davies M. B., Sigurdsson S., 2012, *MNRAS*, 425, 2799

Repetto S., Nelemans G., 2014, *MNRAS*, 444, 542

Repetto S., Nelemans G., 2015, *MNRAS*, 453, 3341

Rocha-Pinto H. J., Flynn C., Scalo J., Häminen J., Maciel W. J., Hensler G., 2004, *A&A*, 423, 517

Sellwood J. A., Preto M., 2002, in Athanassoula E., Bosma A., Mujica R., eds, *Disks of Galaxies: Kinematics, Dynamics and Perturbations* Vol. 275 of *Astronomical Society of the Pacific Conference Series*, *Scattering of Stars by Transient Spiral Waves*. pp 281–292

Takahashi K., Yoshida T., Umeda H., 2013, *ApJ*, 771, 28

Tauris T. M., Langer N., Podsiadlowski P., 2015, *MNRAS*, 451, 2123

Tauris T. M., van den Heuvel E. P. J., 2006, *Formation and evolution of compact stellar X-ray sources*. pp 623–665

Urquhart J. S., Figura C. C., Moore T. J. T., Hoare M. G., Lumsden S. L., Mottram J. C., Thompson M. A., Oudmaijer R. D., 2014, *MNRAS*, 437, 1791

van Paradijs J., White N., 1995, , 447, L33

White N. E., van Paradijs J., 1996, , 473, L25

Willems B., Henninger M., Levin T., Ivanova N., Kalogera V., McGhee K., Timmes F. X., Fryer C. L., 2005, *ApJ*, 625, 324

Wong T.-W., Valsecchi F., Ansari A., Fragos T., Glebbeek E., Kalogera V., McClintock J., 2014, *ApJ*, 790, 119

Wong T.-W., Valsecchi F., Fragos T., Kalogera V., 2012, *ApJ*, 747, 111

Wong T.-W., Willems B., Kalogera V., 2010, *ApJ*, 721, 1689